Science Bulletin xxx (xxxx) xxx

Contents lists available at ScienceDirect

Science Bulletin

journal homepage: www.elsevier.com/locate/scib

Article

The markers and risk stratification model of intracranial aneurysm instability in a large Chinese cohort

Qingyuan Liu [a,b,1], Ke Li [a,1], Hongwei He [a], Zengli Miao [b], Hongtu Cui [d], Jun Wu [a,b], Shusi Ding [a], Zheng Wen [a], Jiyuan Chen [e], Xiaojie Lu [b,*], Jiangan Li [b,*], Lemin Zheng [a,c,*], Shuo Wang [a,b,*]

[a] Department of Neurosurgery, Beijing Tiantan Hospital, China National Clinical Research Center for Neurological Diseases, Advanced Innovation Center for Human Brain Protection, Beijing Institute of Brain Disorders, The Capital Medical University, Beijing 100070, China
[b] Department of Neurosurgery and Emergency Medicine, Jiangnan University Medical Center, Wuxi 214001, China
[c] The Institute of Cardiovascular Sciences and Institute of Systems Biomedicine, School of Basic Medical Sciences, State Key Laboratory of Vascular Homeostasis and Remodeling, NHC Key Laboratory of Cardiovascular Molecular Biology and Regulatory Peptides, Beijing Key Laboratory of Cardiovascular Receptors Research, Health Science Center, Peking University, Beijing 100191, China
[d] Department of Cardiology and Institute of Vascular Medicine, Peking University Third Hospital, Beijing 100191, China
[e] School of Basic Medical Sciences, Fujian Medical University, Fuzhou 350122, China

ARTICLE INFO

Article history:
Received 12 January 2023
Received in revised form 4 April 2023
Accepted 28 April 2023
Available online xxxx

Keywords:
Intracranial aneurysm
Instability
Biomarker
Radiological feature
Risk stratification model

ABSTRACT

Intracranial aneurysm is the leading cause of nontraumatic subarachnoid hemorrhage. Evaluating the unstable (rupture and growth) risk of aneurysms is helpful to guild decision-making for unruptured intracranial aneurysms (UIA). This study aimed to develop a model for risk stratification of UIA instability. The UIA patients from two prospective, longitudinal multicenter Chinese cohorts recruited from January 2017 to January 2022 were set as the derivation cohort and validation cohort. The primary endpoint was UIA instability, comprising aneurysm rupture, growth, or morphology change, during a 2-year follow-up. Intracranial aneurysm samples and corresponding serums from 20 patients were also collected. Metabolomics and cytokine profiling analysis were performed on the derivation cohort (758 single-UIA patients harboring 676 stable UIAs and 82 unstable UIAs). Oleic acid (OA), arachidonic acid (AA), interleukin 1β (IL-1β), and tumor necrosis factor-α (TNF-α) were significantly dysregulated between stable and unstable UIAs. OA and AA exhibited the same dysregulated trends in serums and aneurysm tissues. The feature selection process demonstrated size ratio, irregular shape, OA, AA, IL-1β, and TNF-α as features of UIA instability. A machine-learning stratification model (instability classifier) was constructed based on radiological features and biomarkers, with high accuracy to evaluate UIA instability risk (area under curve (AUC), 0.94). Within the validation cohort (492 single-UIA patients harboring 414 stable UIAs and 78 unstable UIAs), the instability classifier performed well to evaluate the risk of UIA instability (AUC, 0.89). Supplementation of OA and pharmacological inhibition of IL-1β and TNF-α could prevent intracranial aneurysms from rupturing in rat models. This study revealed the markers of UIA instability and provided a risk stratification model, which may guide treatment decision-making for UIAs.

1. Introduction

Intracranial aneurysm (IA) is the leading cause of nontraumatic subarachnoid hemorrhage, with a prevalence of 7% in China [1] and 5% in the United States [2]. More than 70% IAs are unruptured intracranial aneurysms (UIAs), which are incidentally found on imaging [2]. Although aneurysm rupture is associated with high morbidity and mortality, previous studies revealed the rupture rate of UIAs as low as 1% per year [2–4]. Notably, aggressive empirical surgical treatment carries the risk of complications, including ischemic stroke and accidental aneurysm rupture [5]. The key to improving the outcome of UIA patients is determining which UIAs are at risk for rupture, as high-risk UIAs could be referred for surgical treatment, while low-risk UIAs could be observed. Improved identification of UIAs with a high risk of suffering instability (rupture and growth) can better guide treatment decision-making for UIAs.

* Corresponding authors.
E-mail addresses: luxiaojiewuxi@163.com (X. Lu), lijiangan2014@163.com (J. Li), zhengl@bjmu.edu.cn (L. Zheng), captain9858@126.com (S. Wang).
[1] These authors contributed equally to this work.

https://doi.org/10.1016/j.scib.2023.05.001
2095-9273/

Growth has been recognized as the surrogate of IA rupture [4,6]. Therefore, both ruptured and growing (unstable) IAs necessitate surgical intervention. Current models for IA growth and rupture (e.g., PHASES score [7] and ELAPSS score [8]) were established based on clinical and radiological features. Metabolites and cytokines influence the environment of the vessels and are essential for the development of cardiovascular and cerebrovascular diseases [9–11]. Inflammation infiltration and degradation of the extracellular matrix (ECM) are crucial pathological characteristics of ruptured IAs [4,12,13] and contribute to aneurysm growth and rupture [14,15]. A cross-sectional study reported the metabolic difference between patients suffering and not suffering aneurysmal subarachnoid hemorrhage [16]. However, given subarachnoid hemorrhage could affect the metabolic condition [17] and there are few longitudinal studies on the natural history of UIA rupture or growth, the relationship between metabolic-cytokine features and UIA instability was unclear. Moreover, there is a lack of large-scale multi-center longitudinal data in the Chinese population, and most previous studies are limited by small sample size, cross-sectional study design, or single-center cohort [18–20].

In this study, a multi-omics analysis was performed by integrating metabolomics, proteomics, and cytokine profiling, based on two prospective, longitudinal multicenter, Chinese cohort (Intracranial Aneurysm Rupture Prediction in Chinese People cohort (IARP-CP cohort) and online registration cohort for UIAs based on 100 regional medical centers (100-Project cohort)), aiming to investigate the biomarkers related to UIA instability. Subsequently, incorporating radiological features and biomarkers, a risk stratification model of UIA instability was established and validated.

2. Materials and methods

2.1. Study population

This study was approved by the Institutional Review Board of Beijing Tiantan Hospital (KY2022-137-02) and was conducted in compliance with the *Declaration of Helsinki*. All patients (or guardians of patients) provided written informed consents.

The summary of data generation is presented in Fig. 1a. In this study, to investigate the dysregulated metabolites between IA tissues and serums, 20 human IA tissues (including 10 ruptured IAs and 10 unruptured IAs) and corresponding serum samples were prospectively collected from 20 patients between January 2021 and June 2022, as the discovery cohort. The inclusion criteria and exclusion criteria were given in Supplementary methods (online).

To identify the markers of UIA instability and establish a risk stratification model, the radiological and metabolic-cytokine features of UIA patients were analyzed from two prospective, longitudinal multicenter Chinese cohort studies. The patients from the IARP-CP cohort (trial registration: ChiCTR.org; ChiCTR1900024547; enrolling appropriate UIA patients from 8 medical centers between January 2017 to February 2019) and 100-Project cohort (trial registration: ChiCTR.org; ChiCTR2100045705; enrolling appropriate UIA patients from 18 medical centers between September 2021 to May 2022) were set as the derivation cohort (Fig. S1 online) and the validation cohort (Fig. S2 online), respectively. The inclusion criteria and exclusion criteria were given in Supplementary methods (online).

Serum samples were also collected from 31 meningioma patients without pial or cerebral invasion between January 2022 and August 2022 as the healthy control. The inclusion criteria and exclusion criteria were given in Supplementary methods (online).

2.2. Follow-up and the primary endpoint

As illustrated in Fig. 1b, all patients had either digital subtraction angiography or computational tomography angiography (CTA) baseline scans, and additional CTA every 4–6 months during follow-up or until an endpoint event occurred. The details of the management of UIA patients and follow-up were given in Supplementary methods (online).

The primary endpoint was UIA instability, including aneurysm rupture and aneurysm growth (Fig. 1c). The patients must have both the symptoms of subarachnoid hemorrhage (such as severe headache and sudden coma) and imaging evidence on CT or bloody cerebrospinal fluid to identify the rupture events. As illustrated in Fig. S3a (online), aneurysm growth or morphology change during follow-up (compared with baseline) was identified based on criteria established in the previous study [17] as (1) growth of more than 1 mm or 20% in at least one direction, (2) growth of more than 0.5 mm in at least two directions, or (3) new appearance of irregularity on the aneurysm on any imaging follow-ups. Patients with unstable UIA were referred for surgical or endovascular treatment, and their time (months) from baseline to aneurysm growth or rupture was recorded. The final imaging follow-up was 24 months for patients without aneurysm growth or rupture.

2.3. Study design and biomarker discovery

The study design was summarized in Fig. 1d. To identify the markers of UIA instability and establish a risk stratification model for UIA instability, this study included the biomarker discovery, risk stratification model establishment, and *in vivo* validation of biomarkers. We discovered the biomarkers of UIA instability based on the IA tissues and the dynamic change of biomarkers during follow-up (at diagnosis of UIAs versus during follow-up).

Our previous study has revealed the altered cytokines between ruptured IAs and unruptured IAs [21]. In this study, metabolomics analysis was performed on IA tissues. The correlation of metabolites in tissues and serum was also investigated.

To investigate the dynamic change of metabolites and cytokines before and after UIA instability and find the stable biomarkers of UIA instability, the serum samples (at diagnosis of UIAs and during follow-up) of 31 patients with unstable UIAs and 31 patients with stable UIAs were collected from the derivation cohort using propensity score matching. Since subarachnoid hemorrhage may affect the systematic metabolism [17], the biomarkers of UIA instability were investigated based on growing and stable UIAs in the derivation cohort. Propensity score matching was performed to control the effect of clinical-radiological factors related to aneurysm growth and factors related to metabolism (the details are given in Supplementary methods online). The fold change (FC) in serum cytokines and metabolites of unstable UIAs to stable UIAs and variable importance in the project (VIP) was calculated. The metabolites and cytokines, which were co-dysregulated with the same trend at two time points (with $|\log_{1.5}(FC)| > 1$, VIP >1, and $P < 0.05$), were identified as the stable biomarkers of UIA instability. Finally, the stable biomarkers, which also have significance between ruptured IAs and unruptured IAs, were identified as the biomarkers of UIA instability.

2.4. Clinical data and sample collection

The details of clinical data and sample collection were provided in Supplementary methods (online). Radiological characteristics consisted of aneurysm size, aspect ratio, size ratio (SR), regular or irregular shape, and aneurysm location. SR and aspect ratio were

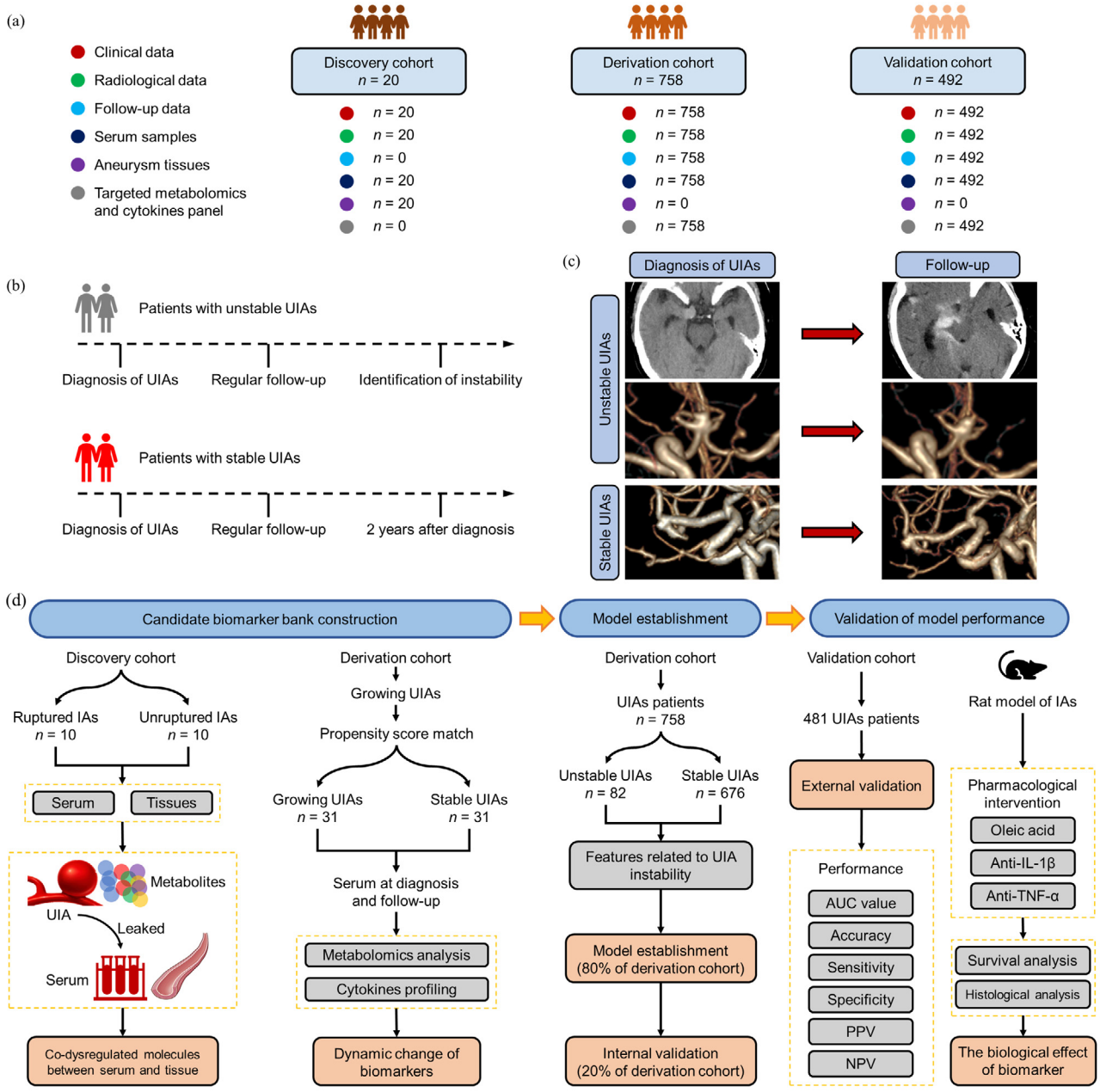

Fig. 1. The diagram of data generation and study design. (a) The summary of data generation. (b) The flow chart of follow-up. We followed up with patients with unstable UIAs until the identification of instability (rupture or growth), as well as patients with stable UIAs until 2 years after diagnosis of UIAs. (c) The baseline and follow-up images of representative cases of unstable UIAs and stable UIAs. (d) The diagram of study design. To identify the markers of UIA instability and establish a risk stratification model for UIA instability, this study included biomarker discovery, risk stratification model establishment, and *in vivo* validation of biomarkers. AUC: area under curve; IA: intracranial aneurysm; NPV: negative predictive value; PPV: positive predictive value; UIA: unruptured intracranial aneurysm.

calculated according to a previous study [22]. According to a previous study [8], the site of UIAs was classified into the anterior cerebral artery (ACA) or anterior communicating artery (Acom), internal carotid artery (ICA), middle cerebral artery (MCA), and posterior communicating artery (Pcom)/posterior circulation. The reproducibility of radiological features was evaluated with Cohen's kappa and intraclass correlation coefficients (Fig. S3b online). PHASES score (with the population, age, hypertension, aneurysm size, aneurysm location, and earlier subarachnoid hemorrhage) and ELPASS score (with the earlier subarachnoid hemorrhage, aneurysm location, age, population, aneurysm size, and irregular shape) was calculated according to previous studies [7,8].

2.5. Cytokines profiling analysis, untargeted metabolomics, and proteomics analysis

The processes and analyses of cytokine profiling analysis, untargeted metabolomics, and proteomics analysis are detailed in Supplementary methods (online).

The metabolomics and proteomics analyses were performed based on the IA tissues. The metabolites and proteins with a $|\log_{1.5}(FC)| > 1$, VIP >1, and $P < 0.05$ between ruptured and unruptured IAs were identified. The Analysis module in MetaboAnalyst (https://www.metaboanalyst.ca/) was used for metabolite classification and pathway enrichment analysis. The ClueGo plug-in in

CytoScape (version 3.6.1) was employed for function enrichment analysis of altered proteins. Enrichment analysis was performed on the Kyoto Encyclopaedia of Genes and Genomes database, and biological process and molecular function were performed on the Gene Ontology database.

The metabolomics and cytokine profiling analyses were performed based on the serums. The FC in serum cytokines and metabolites of unstable UIAs to stable UIAs and VIP was calculated. The cytokines and metabolites with $|\log_{1.5}(FC)|$ >1, VIP >1, and P <0.05 were identified.

2.6. Cytokines panel analysis

The process of cytokines panel analysis was described in Supplementary methods (online). The panel was pre-incubated using the primary antibodies, comprising interleukin 1β (IL-1β), interleukin 1 receptor antagonist (IL-1.ra), monocyte chemoattractant protein 1 (MCP-1), and tumor necrosis factor-α (TNF-α).

2.7. Targeted metabolomics analysis

Targeted metabolomics analysis was performed using multiple reaction monitoring methods. The details of targeted metabolomics analysis were given in Supplementary methods (online). The expression level of oleic acid (OA), arachidonic acid (AA), α-linoleic acid (ALA), eicosapentaenoic acid (EPA), docosahexaenoic acid (DHA), and chenodeoxycholic acid disulfate (CAD) was detected.

2.8. Machine-learning model

The machine-learning model creation was detailed in Supplementary methods (online). A learning curve of instability classifier was plotted based on the area under curve (AUC) to evaluate for overfitting [23]. The accuracy, specificity, sensitivity, positive predictive value (PPV), and negative predictive value (NPV) of the instability classifier in classifying unstable UIAs and stable UIAs were further calculated.

2.9. Rat model of IA and in vivo intervention

The IA model was constructed based on the DOCA (desoxycorticosterone acetate)-hypertension model using the operation plus β-aminopropionitrile, which was also used in the previous study [24]. The details of constructing a rat model of IA and histological analysis were presented in Supplementary methods (online). 9- to 10-week male Sprague Dawley rats were purchased from Vitalriver Corporation (Charles River co-partnership Co, Ltd., Beijing, China), all of which were included in this study. The protocol of animal studies was approved by the Animal Care and Use Committee of Chinese Neurosurgical Institution (202003005), and these studies were conducted in compliance with the *National Institutes of Health Guide for the Care and Use of Laboratory Animals*. With respect to the pharmacological intervention, from the 5th d to the 28th d after the operation, rats received a subcutaneous injection of Adalimumab (2 mg/kg, monoclonal antibody for TNF-α) [25] and Canakinumab (10 mg/kg, monoclonal antibody for IL-1β) [26] once a week for 3 weeks, and 0.1 mL of OA was supplemented by gavage per day. Moreover, rats receiving a subcutaneous injection of physiological saline (control 1) and receiving physiological saline (control 2) by gavage were set as the control.

2.10. Statistical analysis

The statistical analyses were conducted with SPSS (version 24.0, SPSS Co., Chicago, USA). A two-sided P <0.05 was recognized as statistical significance. Continuous variables with normal distribution were presented as means and standard deviation, and medians (m) and inter-quartile range (IQR) if the data were not normally distributed. Categorical variables were presented as numbers (n) and percentages (%). The differences in continuous variables were compared using Student's t-tests or Wilcoxon rank sum tests, and the differences in categorical variables were analyzed using Chi-square tests or Fisher's exact tests. The correlation of metabolites between IA tissues and serum was tested using the Pearson correlation analysis. The result was presented as the square of the correlation coefficient (R^2) and P. Univariate Cox regression analyses were performed to identify the risk factors of UIA instability. A multivariate Cox regression model was further conducted on the factors with significance in univariate analyses to demonstrate the factors related to UIA instability independently, using the backward method. Survival analyses were performed to compare the risk of UIA instability between the high-risk and low-risk groups stratified by instability classifier and among rat models of IA receiving different treatments, using the Kaplan-Meier method and log-rank test. The accuracy of models for UIA instability was evaluated by using the AUC and receiver operator characteristic curve (ROC). The model with an AUC >0.8 as having clinical utility. The AUC value and accuracy were compared using the Z-test.

Subgroup analysis was performed to identify whether an instability classifier can evaluate the risk of UIA instability, after controlling the effect of modified factors for UIA growth and rupture (age, gender, smoker, aneurysm location and size, aspirin, and statin usage) [7,8] and potential factors related to metabolism (Han people, geographic region, dyslipidemia, and diabetes mellitus).

A sensitivity analysis was performed to investigate the importance of metabolites and cytokines in evaluating the risk of UIA instability. Three models (model 1, based on radiological features; model 2, based on metabolites and cytokines; model 3, based on all features) were established using the random forest (RF) algorithm. The AUC value and accuracy of three models to evaluate the risk of UIA instability were compared using the Z-test. The net reclassification improvement (NRI) was further evaluated, and discrimination improvement (IDI) of model 3 to model 1, and model 3 to model 2, was integrated according to a previous study [27]. If NRI or IDI was >0, the predictive ability of the model was improved.

3. Results

3.1. The disorder of lipid metabolism is related to IA rupture (instability)

Metabolomics and proteomics analyses were performed on 20 IA tissues in the discovery cohort (including 10 unruptured IAs and 10 ruptured IAs, Fig. 2a). The information of patients in the discovery cohort was given in Table S1 (online). Among them, the median age was 57 years (range, 46–71 years); 12 (60.0%) were male.

Untargeted metabolomics analysis identified 38 altered metabolites, including OA, AA, and ALA, between ruptured and unruptured IAs (Fig. 2b). Subsequent targeted metabolomics analysis demonstrated that AA was upregulated, and OA was downregulated in the ruptured IAs (Fig. 2c). Moreover, targeted metabolomics analysis also found significance on ALA between ruptured and unruptured IAs (Fig. S4a online). Altered metabolites were primarily lipid and lipid-like molecules (Fig. 2d) and enriched in the biosynthesis of the unsaturated fatty acid pathway (Fig. S4b online). AA and OA in the IA tissues performed well to classify ruptured IAs from unruptured IAs (Fig. 2e). Subsequently, targeted metabolomics analysis implied a strong consistency of AA and

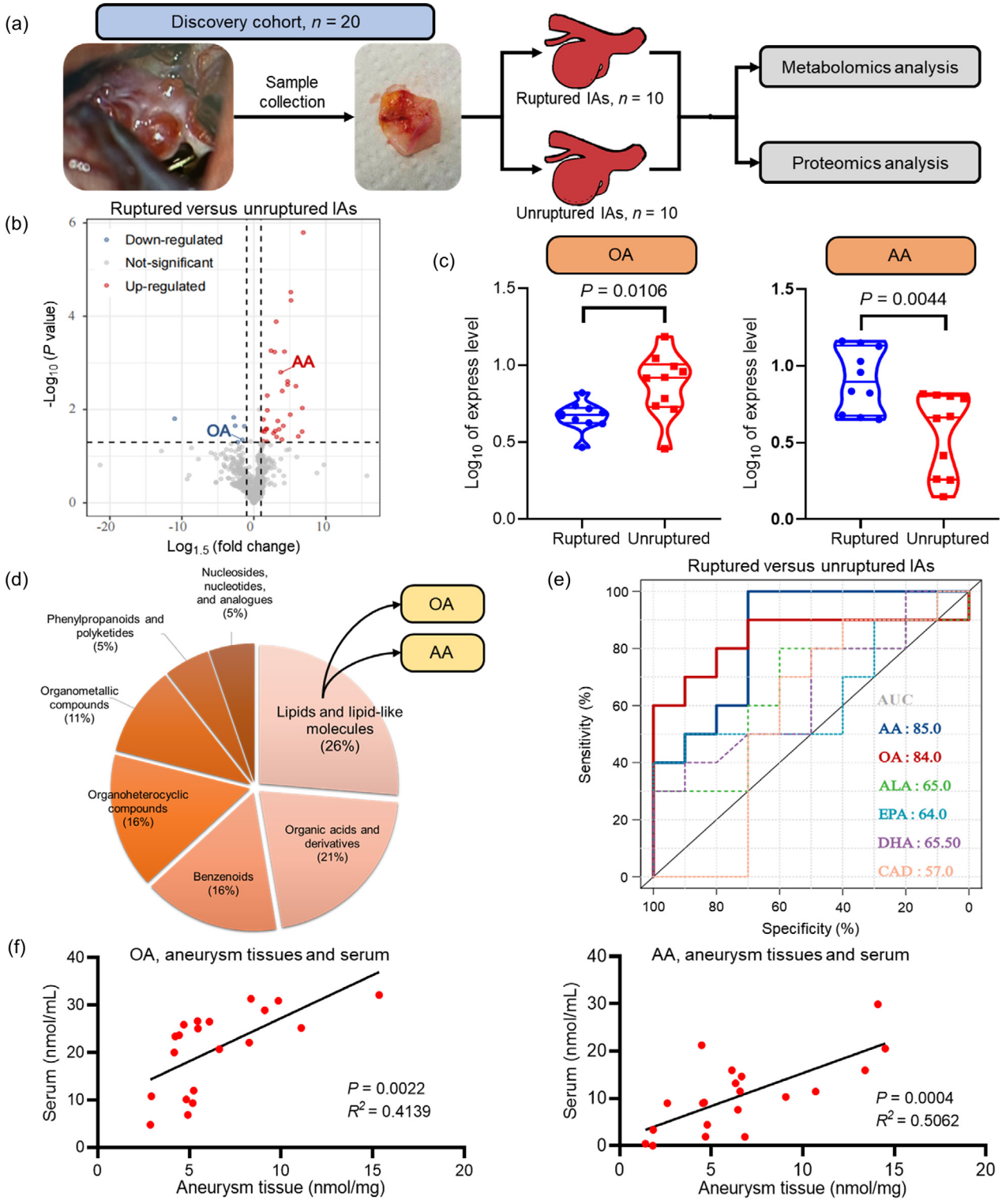

Fig. 2. Dysregulated metabolites in IA tissues and serum. (a) The flowchart of metabolomics analysis based on human IA tissues. (b) The volcano plot presents the result of untargeted metabolomics based on human IA tissues. 38 metabolites were altered between ruptured and unruptured IAs. (c) The violin plots present the result of targeted metabolomics for AA and OA, based on human IA tissues. OA and AA were significantly different between ruptured and unruptured IAs. (d) Altered metabolites between ruptured and unruptured IAs were mainly lipids and lipid-like molecules. OA and AA were lipids and lipid-like molecules. (e) The ROC curves present the accuracy of each metabolite to discriminate ruptured IAs from unruptured IAs. (f) The scatter plots present the correlation of OA and AA between IA tissues and serum. There was a good correlation of OA and AA between IA tissues and serum. AA: arachidonic acid; ALA: α-linoleic acid; AUC: area under curve; CAD: chenodeoxycholic acid disulfate; DHA: docosahexaenoic acid; EPA: eicosapentaenoic acid; IA: intracranial aneurysm; OA: oleic acid; ROC: receiver operator characteristic.

OA (Fig. 2f) between IA tissue and serum. However, there was no consistency of DHA and CAD between IA tissue and serum (Fig. S4c online).

Increasing expression of matrix metalloproteinases (MMPs) and degradation of ECM plays essential roles in the development of IA rupture [13,28,29]. Thus, MMPs and collagens are proteins of IA

rupture. Proteomics analysis found 571 altered proteins, including MMP2, MMP9, collagen type 1A1 (COL1A1), and collagen type 1A2 (COL1A2), between ruptured and unruptured IAs (Fig. S5a online). Altered protein majorly enriched in metabolic pathways (Fig. S5b online) and regulated the metabolism of ECM (Fig. S5c online). A strong correlation was identified among AA, MMP9, MMP2, and COL1A1, and among OA, MMP2, COL1A1, and COL1A2 (Fig. S5d online). 11 enzymes related to the biosynthesis of the unsaturated fatty acid pathway were significantly different between ruptured and unruptured IAs (Fig. S5e online), and interacted with the rupture-related proteins (Fig. S5f online). AA and OA participated in the biosynthesis of the unsaturated fatty acid pathway.

In sum, these findings suggested that the abnormity of lipid metabolism is related to IA rupture, and OA and AA may serve as serum biomarkers for UIA instability.

3.2. Establishment of the biomarker bank for UIA instability

After a mean follow-up duration of 23.0 ± 3.6 months (range, 1.3–24.0 months), the derivation cohort included 758 patients harboring 758 UIAs. During 2021.8 person-years of follow-up, UIA instability occurred in 82 patients (10.8%), consisting of 58 patients with growth and 24 with rupture. Patient data of the derivation cohort were given in Table S2 (online). For all included patients, the median age was 55 years, and 332 (42.6%) were male. For all UIAs, the median size was 3.9 mm (range, 3.0–33.2 mm). 139 (18.3%) UIAs had an irregular shape.

The above analysis based on the IA tissues showed that the lipid metabolism disorder is related to IA rupture. Our previous study showed that cytokines (e.g., IL-1β and TNF-α) were also related to IA instability [21]. After controlling the effect of the metabolic difference caused by daily living [30] and clinical-radiological factors related to aneurysm growth [7,8], metabolomics and cytokine profiling analyses were performed on serum samples of 31 patients with stable UIAs and 31 patients with growing UIAs (unstable) from the derivation cohort (Fig. 3a), yielded by the propensity score matching (Fig. S6a online). The score before and after matching was given in Fig. S6b (online). The information of these 62 UIA patients and healthy controls was given in Table S3 (online). As shown in Fig. 3b, untargeted metabolomics analysis identified 117 altered metabolites at diagnosis of UIAs, and 79 altered metabolites during follow-up of UIAs, between patients with stable and unstable UIAs (also seen in Fig. S6c online). OA, AA, ALA, EPA, DHA, and CAD were significantly dysregulated at different time points between patients with stable and unstable UIAs, which were mainly lipids and lipid-like molecules (Fig. S6d online), and participated in the biosynthesis of unsaturated fatty acid pathway and linoleic acid metabolism pathway (Fig. S6e–f online). AA and OA are mainly involved in the biosynthesis of the unsaturated fatty acid pathway (Fig. S6f online). Moreover, cytokine profiling analysis identified 6 altered cytokines (including IL-1β, IL-1.ra, MCP-1, TNF-α, growth-regulated oncogene-α (GRO-α), and TNF-related apoptosis-inducing ligand (TRAIL)) at diagnosis of UIAs, and 4 altered cytokines (including IL-1β, IL-1.ra, MCP-1, and TNF-α) during follow-up of UIAs, between patients with stable and unstable UIAs (Fig. 3c). IL-1β, IL-1.ra, MCP-1, and TNF-α were dysregulated at different time points between patients with stable and unstable UIAs. Generally, metabolomics analysis based on IA tissues and the dynamic change of metabolites on serum showed three metabolites, including OA, AA, and ALA, with significant differences among patients with stable UIAs. Thus, we included these three metabolites (OA, AA, and ALA) and four cytokines (IL-1β, IL-1.ra, MCP-1, and TNF-α) as the biomarker bank for UIA instability (Fig. 3d). OA, AA, and ALA were lipids and lipid-like molecules (Fig. 3e), which is related to atherosclerosis [31]. The biological function of IL-1β, MCP-1, and TNF-α was proinflammatory, and IL-1.ra worked as the anti-inflammatory cytokine (Fig. 3e).

The difference in seven biomarkers between stable and unstable UIAs was further verified based on the population-based cohort (758 patients in the derivation cohort). Targeted metabolomics and cytokine panel analysis implied that OA, AA, IL-1β, IL-1.ra, and TNF-α were significantly changed (Fig. 4a), whereas no significant difference was found in MCP-1 and ALA (Fig. S7 online), between patients with stable and unstable UIAs. There was an increasing trend of AA, IL-1β, and TNF-α, and a decreasing trend of OA among stable UIAs, growing UIAs, and ruptured UIAs (Fig. S8a online).

Thus, based on these facts, OA, AA, IL-1β, IL-1.ra, and TNF-α were reliable biomarkers to evaluate the risk of UIA instability.

3.3. Risk stratification model for UIA instability

The features of UIA instability were further investigated based on the derivation cohort. Besides OA, AA, IL-1β, IL-1.ra, and TNF-α, a significant difference was also observed in hypertension, aneurysm location and size, aspect ratio, SR, bifurcation configuration, and irregular shape, between unstable UIAs and stable UIAs (all P <0.05, Table S2 online). Univariate (Table S4 online) and multivariate (Table S5 online) Cox regression analysis revealed irregular shape, high SR, increasing AA, decreasing OA, increasing IL-1β, and increasing TNF-α as risk factors of UIA instability; LASSO regression analysis also showed irregular shape, SR, AA, OA, IL-1β, and TNF-α as features of UIA instability (Fig. S8b online).

Incorporating two radiological features and four biomarkers, risk stratification models were further established using the machine-learning algorithms and selected the best-performing model (with the highest AUC) as the instability classifier (Fig. 4b). Among these classification models (Fig. 4c), the RF model performed best to classify unstable UIA and stable UIAs, which was superior to the Coxboost model and support vector machine (SVM) model (AUC, 0.94 vs. 0.82 and 0.86; P <0.001), within the derivation cohort. The performance of the RF model in classifying stable UIAs from unstable UIAs was presented in Fig. 4d, and the performance of the Coxboost model and SVM model was presented in Fig. S8c (online). According to the accuracy of models in classifying stable UIAs and unstable UIAs within the derivation cohort, the RF model had the highest accuracy, followed by the Coxboost model and SVM model (accuracy, 0.97 vs. 0.90 and 0.82; P <0.001). Based on the above findings, the RF model was selected as the instability classifier. The importance of each parameter in the RF model was given in Fig. S8d (online). The learning curves suggested that there was no overfitting issue in the RF model (Fig. S8e online). The performance of the instability classifier in classifying unstable from stable UIAs was summarized in Table S6.

The patients in the high-risk group stratified by the instability classifier had a higher risk of suffering UIA instability compared with the patients in the low-risk group (Fig. 4e). Within the derivation cohort, our instability classifier was superior to the PHASES and ELAPSS score in evaluating the risk of UIA instability (AUC, 0.94 vs. 0.70 and 0.67, P <0.001; Fig. 4f), or evaluating the risk of UIA growth (AUC, 0.92 vs. 0.68 and 0.62, P <0.001; Fig. S8f online), or evaluating the risk of UIA rupture (AUC, 0.99 vs. 0.70 and 0.73, P <0.001; Fig. S8g online). The subgroup analysis showed that, after controlling effects from the modified factors of aneurysm rupture or growth and factors related to metabolism, patients in the high-risk group stratified by instability classifier still had a higher risk of UIA instability compared with patients in the low-risk group (Fig. S9 online).

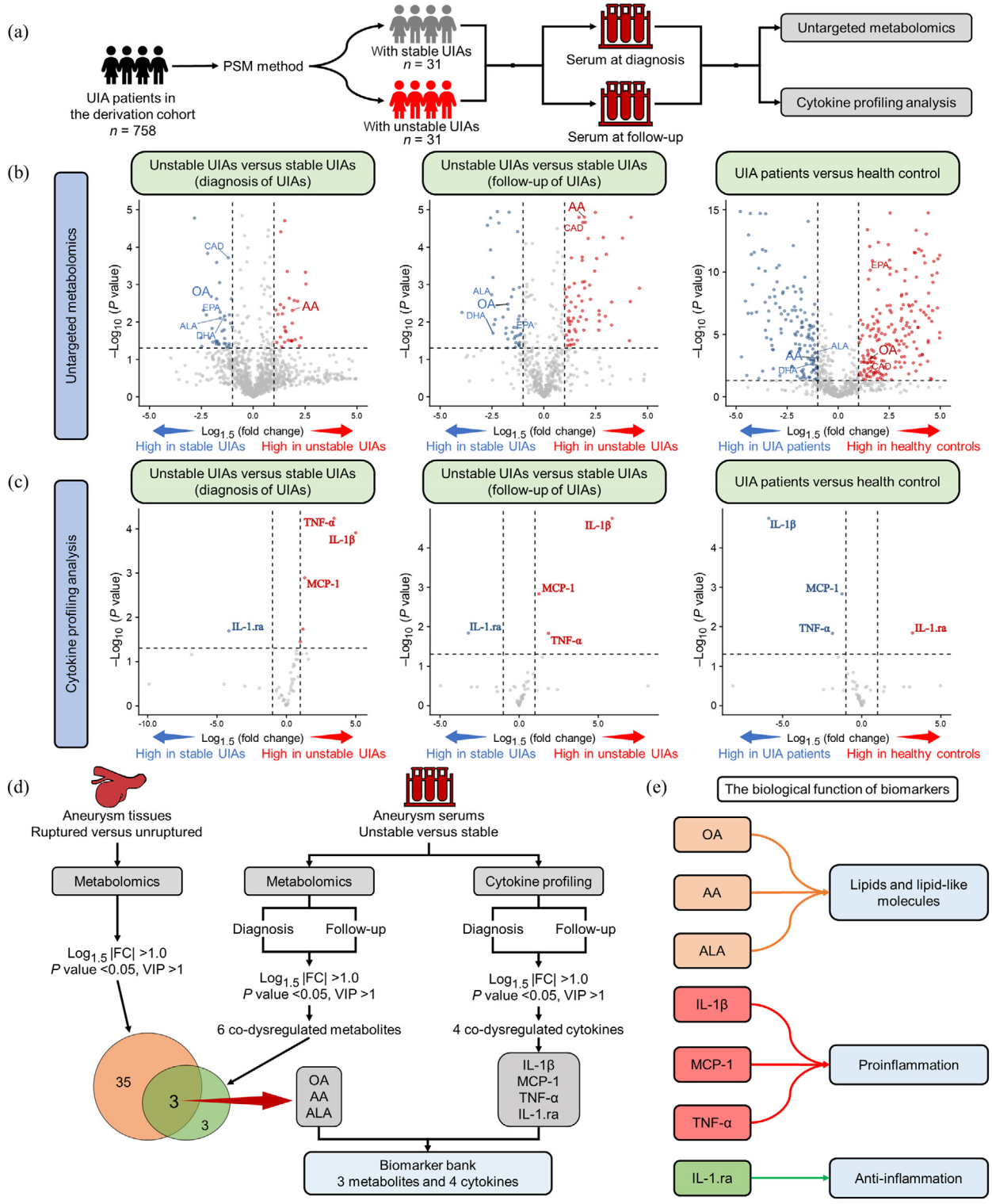

Fig. 3. Biomarker discovery and biomarker bank of UIA instability. (a) The diagram of metabolomics and cytokine profiling analysis on serums to investigate the dynamic change of biomarkers and identify the stable biomarkers of UIA instability. (b) The volcano plots reveal the altered metabolites between growing (unstable) and stable UIAs at different time points (at diagnosis of UIAs and during follow-up), and between healthy control and UIA patients (at diagnosis of UIAs). (c) The volcano plots present the altered cytokines between growing (unstable) and stable UIAs at different time points (at diagnosis of UIAs and during follow-up), and between healthy control and UIA patients (at diagnosis of UIAs). (d) The diagram of establishing the biomarker bank for UIA instability. Finally, three metabolites and four cytokines were included as the biomarker bank for UIA instability. (e) The biological function of molecules in the biomarker bank for UIA instability. OA, AA, and ALA were lipids and lipid-like molecules. IL-1β, MCP-1, and TNF-α were proinflammatory cytokines, and IL-1.ra is an anti-inflammatory cytokine. AA: arachidonic acid; ALA: α-linoleic acid; IL-1β: interleukin 1β; IL-1.ra: interleukin 1 receptor antagonist; MCP-1: monocyte chemoattractant protein 1; OA: oleic acid; PSM: propensity score matching; TNF-α: tumor necrosis factor α; UIA: unruptured intracranial aneurysm. A, arachidonic acid; ALA.

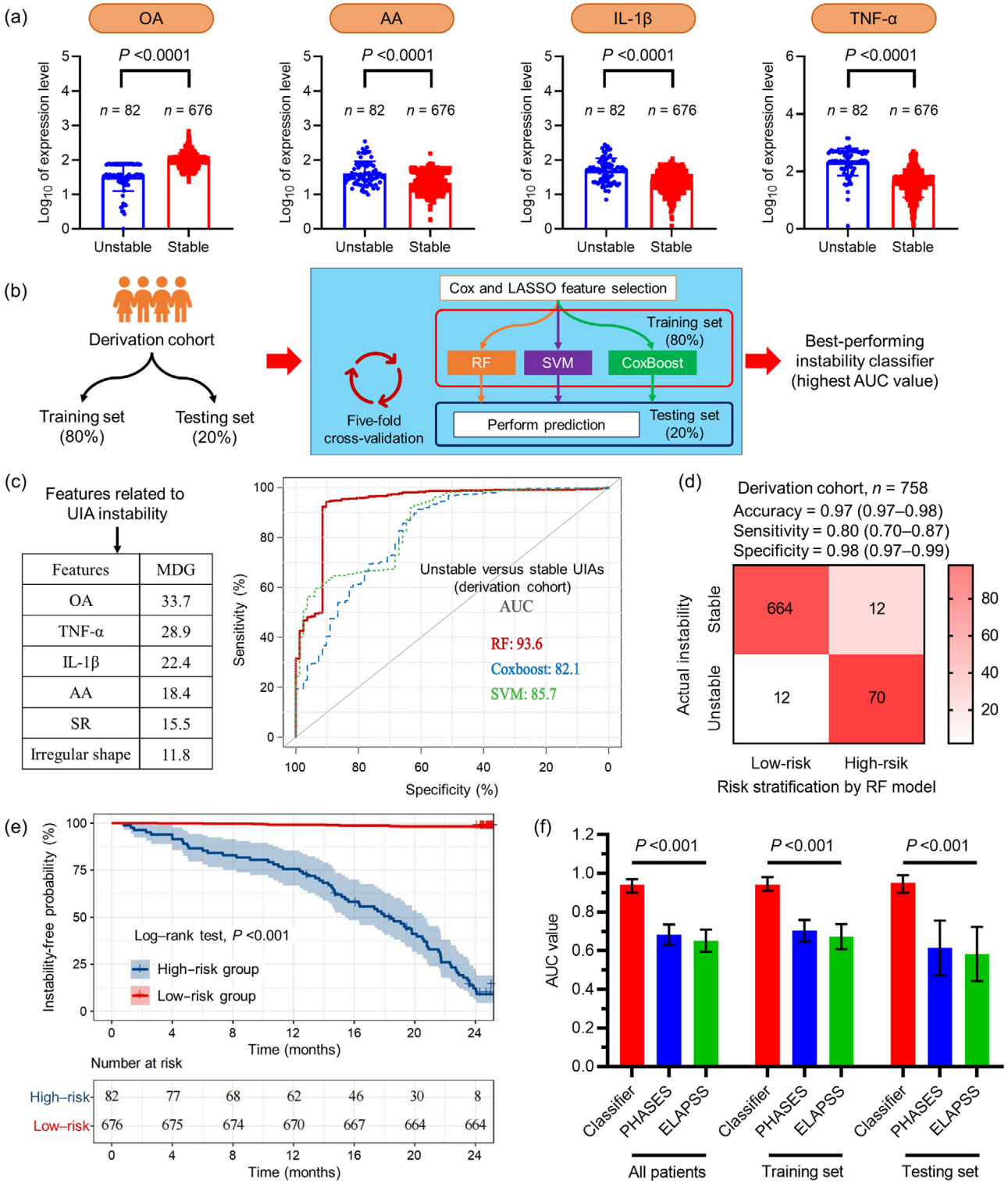

Fig. 4. Risk stratification model for UIA instability. (a) The histograms exhibit the result of targeted metabolomics and cytokine panel analysis based on the derivation cohort (n = 758). OA, AA, IL-1β, and TNF-α were significantly different between unstable and stable UIAs. (b) The diagram of the establishment of risk stratification model for UIA instability. (c) The importance of features related to UIA instability, and the performance of each model to discriminate unstable UIAs from stable UIAs. The importance of features related to UIA instability was evaluated using MDG. The RF model had the highest accuracy to identify unstable UIAs, followed by the SVM model and Coxboost model. (d) The confusion matrix shows the performance of the RF model in classifying unstable UIAs and stable UIAs. (e) Survival curves present the risk of UIA instability in the high-risk group and low-risk group stratified by the instability classifier. (f) The histograms present the AUC value of the instability classifier, PHASES score, and ELAPSS score to evaluate the risk of UIA instability within the derivation cohort. The instability classifier had the highest AUC to evaluate the risk of UIA instability, followed by the PHASES score and ELAPSS score. AA: arachidonic acid; ALA: α-linoleic acid; AUC: area under curve; IL-1β: interleukin 1β; MCP-1: monocyte chemoattractant protein 1; MDG: mean decrease Gini; OA: oleic acid; PSM: propensity score matching; RF: random forest; SVM: support vector machine; TNF-α: tumor necrosis factor α; UIA: unruptured intracranial aneurysm.

3.4. External validation of the performance of the instability classifier

To validate the performance of the instability classifier, external validation was conducted based on the validation cohort (including 492 UIA patients). During 908.4 person-years of follow-up, UIA instability occurred in 76 (15.4%) patients, comprising 10 ruptures and 66 growths. The information of patients in the validation cohort was given in Table S7 (online). Of all included patients, 227 (46.1%) patients were male, and the median age was 55. Besides, the median aneurysm size was 5.7 mm, and 97 (19.7%) UIAs were irregular.

The evaluation process and images of two representative cases were presented in Fig. 5a. The Cox analysis demonstrated irregular shape, larger SR, decreasing OA, increasing AA, increasing IL-1β, and increasing TNF-α as the risk factors related to UIA instability independently (Table S8 online). Instability classifier identified 74 (15.0%) UIAs and 418 (85.0%) UIAs as high-risk and low-risk, respectively; and, the accuracy of the instability classifier in classifying unstable and stable UIAs was 0.94 (Fig. 5b, also seen in Table S6 online). The patients in the high-risk group stratified by the instability classifier had a higher risk of suffering from UIA instability (Fig. 5c). Instability classifier performed well to evaluate the risk of UIA instability, which was superior to the PHASES score and ELAPSS score (AUC, 0.89 vs. 0.73 and 0.73, P <0.001; Fig. 5d).

Subsequent subgroup analysis showed that, after controlling the modified factors related to aneurysm growth and rupture and factors related to metabolism, the high-risk patients stratified by the instability classifier also had a higher risk of UIA instability compared with the low-risk patients (Fig. S10 online). Thus, based on the above findings, the instability classifier had a good accuracy to evaluate the risk of UIA instability and could stratify UIA patients into the high-risk and the low-risk. The cumulative incidence of 2-year instability was 83.3 per 100 persons for high-risk patients and 2.6 per 100 persons for low-risk patients (Fig. 5e).

3.5. Sensitivity analysis of metabolic-cytokine features for UIA instability

To highlight the importance of metabolites and cytokines in evaluating the risk of UIA instability, we further performed sensitivity analysis and established three models (Fig. S11a online). The performance of three models in classifying unstable and stable UIAs within the derivation cohort and validation cohort was illustrated in Fig. S11b (online). Based on all 1250 UIA patients, model 3 (based on radiological features and metabolic-cytokine features) had the highest AUC value to evaluate the risk of UIA instability, followed by model 2 (based on metabolic-cytokine features) and model 1 (based on radiological features) (AUC, 0.93 vs. 0.82 and 0.74, P <0.001; Fig. S11c online). This result was also confirmed on the accuracy of models to evaluate the risk of UIA instability (accuracy, 0.96 vs. 0.88 and 0.86, P <0.001; Fig. S11c online).

As shown in Table S9 (online), the NRI and IDI of model 3 to model 1 were 0.73 (P <0.001) and 0.78 (P <0.001), suggesting that metabolic-cytokine features could improve the ability of radiological features to classifying unstable and stable UIAs. Moreover, the NRI and IDI of model 3 to model 2 were 0.33 (P <0.001) and 0.29 (P = 0.003), also suggesting that there was a complementarity between radiological features and metabolic-cytokine features in evaluating the risk of UIA instability.

3.6. In vivo intervention of OA, IL-1β, and TNF-α could prevent IA from rupture

Whether *in vivo* intervention of OA, IL-1β, and TNF-α could prevent IA from rupture was further investigated (Fig. 6a). Because AA usually could not be supplied by exogenous pure AA, whether the intervention of AA is related to a lower incidence of IA rupture wasn't further investigated. Adalimumab is the monoclonal antibody for TNF-α [25], and Canakinumab is the monoclonal antibody for IL-1β [26].

The blood pressure had no significant difference among the groups (Fig. S12a online). On the 14th d after surgery, IAs occurred in 80% of DOCA-hypertension rats (Fig. S12b online). The incidence of IA rupture was approximately 60% in these rats with IAs (Fig. S12c online). The images from representative cases of ruptured and unruptured IAs were presented in Fig. 6b (also seen in Fig. S12d online). Compared with the gavage controls (control 1), the rats receiving supplementation of OA had a lower risk of IA rupture (Fig. 6c). Moreover, compared with the injection controls (control 2), the rats receiving specific inhibitors of IL-1β or TNF-α also had a lower risk of IA rupture (Fig. 6d).

Activation of the inflammation pathway (such as the nuclear factor kappa B1 (NFKB1) pathway) plays a critical role in IA rupture [13,15]. Thus, whether the intervention of OA, IL-1β, and TNF-α could inhibit the expression of MMP2 and NFKB1 was explored. Supplementation of OA and inhibition of IL-1β or TNF-α inhibited the expression of MMP2 and NFKB1 (Fig. 6e and Fig. S12e online). These findings supported the role of OA, IL-1β, and TNF-α as the biomarkers for UIA instability, and the utility of instability classifier to evaluate the risk of UIA instability.

4. Discussion

This study demonstrated that AA, OA, IL-1β, and TNF-α were significantly dysregulated between stable and unstable UIAs and could serve as biomarkers for UIA instability. The instability classifier, incorporating radiological features and biomarkers, presented a high accuracy in evaluating the risk of UIA instability and contributed to UIA risk stratification, which was superior to the PHASES score and ELAPSS score. To our best knowledge, this is the first and largest longitudinal multi-center study in Chinses patients with UIAs to investigate the radiological and biological markers of UIA instability.

Metabolic and cytokine conditions may be affected by daily living and diseases (such as infection and chronic inflammation) [30,32,33]. There was a lack of large-scale longitudinal data in China to identify biomarkers to predict UIA instability. To control the effect of daily living and diseases, this study analyzed the correlation of metabolites and cytokines between aneurysm tissues and serum to identify specific biomarkers of UIA instability. The change of metabolites and cytokines before and after aneurysm growth was also investigated to find stable biomarkers for UIA instability based on two longitudinal, multicenter studies. Thus, this study could provide a deep understanding of biomarkers for predicting UIA instability.

This study identified lipid molecules and proinflammatory cytokines as serum biomarkers related to UIA instability. Atherosclerotic remodeling is one of the vital pathological characteristics of ruptured IAs [14,28,29]. Metabolites can participate in the origin and development of vascular inflammation [9]. This study unveiled that lipid metabolism disorder, which is also essential for the development of atherosclerosis [32,34], was the prominent characteristic of patients with unstable UIAs. AA and OA were lipid molecules. Previous studies reported that AA metabolism was associated with the development of cerebrovascular and cardiological diseases [10,35,36]. Our data revealed that AA was upregulated in the unstable UIAs, which was the substrate of cyclooxygenase-1 as an oxidative metabolite. Notably, inhibition of cyclooxygenase-1 curtailed the inflammation in the aneurysm wall [37]. Moreover, our data also showed that OA was downregulated in unstable UIAs, which could serve as an angiogenesis initiator to promote the pro-

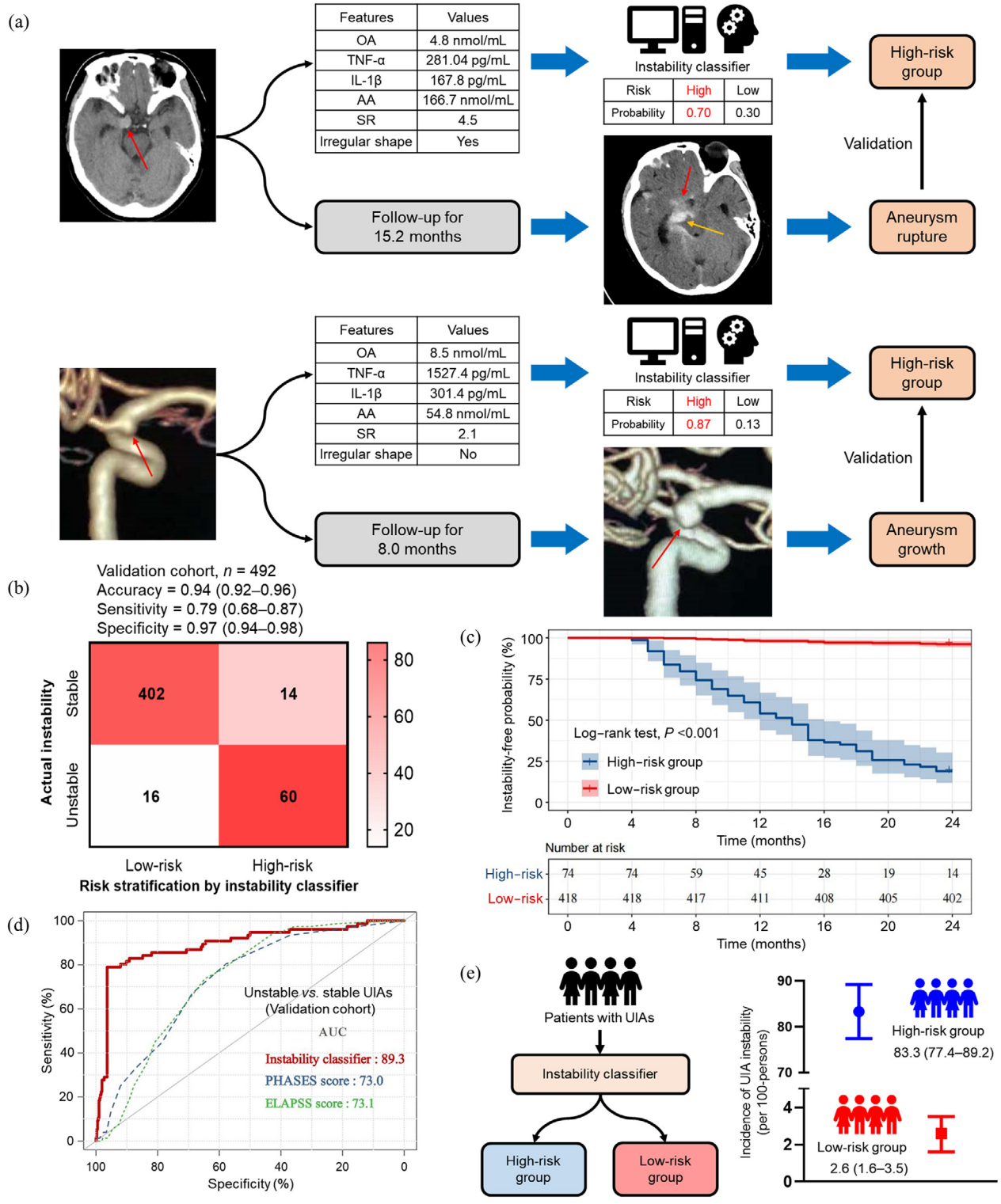

Fig. 5. Validation of the performance of instability classifier for UIA instability. (a) The evaluation process and images of two representative cases which were stratified as high-risk by the instability classifier. The red arrows indicate UIAs, and the orange arrow indicates subarachnoid hemorrhage. (b) The confusion matrix presents the performance of the instability classifier in classifying stable and unstable UIAs. (c) Survival curves illustrate the risk of UIA instability in the high-risk group and low-risk group stratified by the instability classifier. (d) The ROC curves of models to evaluate the risk of UIA instability. The instability classifier had the highest AUC value to evaluate the risk of UIA instability, followed by the PHASES score and ELAPSS score. (e) The summary of instability classifier. The instability classifier could stratify UIA patients into high-risk and low-risk groups. The 2-year cumulative incidence of UIA instability was 83.3 per 100 persons for high-risk patients and 2.6 per 100 persons for low-risk patients. AA: arachidonic acid; AUC: area under curve; IL-1β: interleukin 1β; OA: oleic acid; ROC: receiver operator characteristic; SR: size ratio; TNF-α: tumor necrosis factor α; UIA: unruptured intracranial aneurysm.

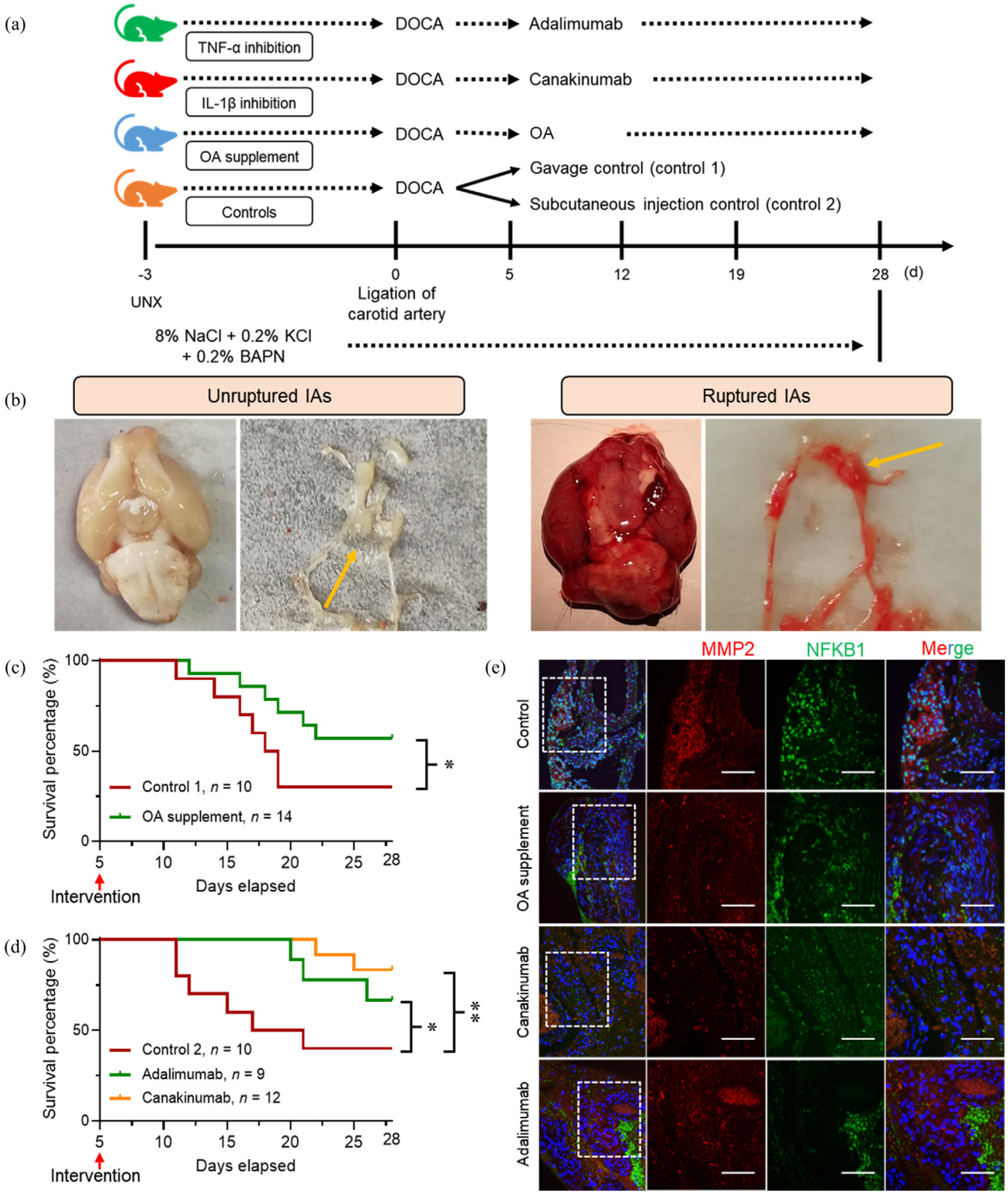

Fig. 6. Intervention of OA, IL-1β, and TNF-α could prevent IA from rupture. (a) The diagram of establishing rat model of IAs and pharmacological intervention. Adalimumab is the specific inhibitor for TNF-α, and canakinumab is the specific inhibitor for IL-1β. (b) Pathological images of representative cases of ruptured and unruptured IAs. (c) Survival analysis suggested that supplementation of OA can prevent IAs from rupture. Rats receiving supplementation of OA (n = 14) had a lower risk of IA rupture compared with the gavage controls (control 1, n = 10). (d) Survival analysis suggested that pharmacological inhibition of TNF-α or IL-1β can prevent IAs from rupture. Rats receiving Adalimumab (n = 9) or rats receiving canakinumab (n = 12) had a lower risk of IA rupture compared with the injection controls (control 2, n = 10). (e) The immunofluorescence of representative cases. The control group had the highest expression of MMP2 and NFKB1. Supplementation of OA and pharmacological inhibition of IL-1β or TNF-α can inhibit the expression of MMP2 and NFKB1. Scale bar: 50 μm. * P <0.05; ** P <0.001. BAPN: β-aminopropionitrile; DOCA: desoxycorticosterone acetate; IA: intracranial aneurysm; IL-1β: interleukin 1β; MMP2: matrix metalloproteinase 2; NFKB1: nuclear factor kappa B1; OA: oleic acid; TNF-α: tumor necrosis factor α; UNX: uni-nephrectomy.

liferation of smooth muscle cells and inhibit inflammation [38,39]. Another finding was that OA and AA were correlated to rupture-related proteins (MMPs and collagens) in aneurysm tissues. Thus, AA and OA metabolism are related to UIA instability. Additionally, inflammation infiltration is another important pathological characteristic of a ruptured aneurysm [14,28,29,40]. This study showed that proinflammatory cytokines, i.e., IL-1β and TNF-α, were elevated in patients with unstable UIAs. IL-1β has been reported as a crucial factor of pyroptosis [41–43]. As indicated by previous studies [21,44], the IL-1β in UIAs may parallel systemic IL-1β changes and could evaluate the risk of UIA instability. A previous study showed that IL-1β deficiency may prevent UIA formation [45]. In addition, TNF-α refers to a pro-inflammatory factor for IAs, which can induce macrophage polarization and cause atherosclerosis formation [46]. Disruption of pro- and anti-inflammatory balance can contribute to atherosclerotic remodeling [47] and UIA instability [48]. Thus, IL-1β and TNF-α could evaluate the risk of UIA instability. Subsequent *in vivo* study using a rat model of IA highlighted the intervention of OA, IL-1β, and TNF-α could prevent IA from rupture, consistent with the result of clinical follow-up. Generally, AA, OA, IL-1β, and TNF-α could serve as serum biomarkers to evaluate the risk of UIA instability and may be the new therapeutic targets to prevent IAs from rupture. However, this study didn't identify the disorder in glutathione or bile acid metabolism, as reported by a recent study [16]. This may due to the difference in patients' status (the natural history of UIAs vs. the cross-sectional study on ruptured and unruptured IAs, because subarachnoid hemorrhage could affect the metabolic status [17]) and studied samples (IA tissues and plasma vs. only plasma).

This study also revealed SR and irregular shape as features of UIA instability. SR can reflect the relative size of UIAs by considering the diameter of the parent arteries [19,22], which maybe a better indicator of unstable risk than the absolute size of the UIA [20,49]. The size was not an independent risk factor for UIA instability when SR was included in the model, which was consistent with previous studies [20,50,51]. The irregular shape usually suggested the imbalance condition within the aneurysm and fragile points in the wall [48,52]. This study did not find age and aneurysm location as independent factors of UIA instability, which was included in PHASES and ELAPSS scores [7,8]. This may be due to the difference in the studied population (Chinese vs. Japanese/North American/European).

Accurate identification of UIAs at high risk of instability can better guide the management of UIA patients. In this study, the instability classifier, comprised of radiological features (irregular shape and SR) and biomarkers (AA, OA, IL-1β, and TNF-α) was further established for risk stratification for UIA instability. Our data presented a complementarity between radiological features and metabolic-cytokine features in evaluating the risk of UIA instability. The instability classifier provided a comprehensive understanding of the radiological and metabolic-cytokine features of unstable UIAs. Thus, this model was superior to the ELAPSS score and PHASES score which only considered clinical and radiological features. The 2-year incidence of UIA instability was 83.3 per 100 persons for the high-risk patients stratified by instability classifier, which was at least ten times higher compared with the low-risk group (2.6 per 100 persons). For patients stratified as high-risk, surgical or endovascular treatment should be immediately recommended, to prevent UIA rupture; and, for patients stratified as the low-risk, given patients may not benefit from surgery, conservative management could be considered. Thus, our instability classifier could help treatment decision-making for UIAs. Its value in other populations is still pending validations.

The strengths of this study are as follows: (1) This might be the first and largest multi-omics study based on the Chinese population to investigate the biomarkers of UIA instability. (2) Based on the correlation of metabolites between IA tissues and serums, and the dynamic change of metabolites and cytokines at different time points, this study identified the specific and stable biomarkers of UIA instability. (3) A risk stratification model was constructed to identify the patients with high-risk UIAs with high accuracy, which may help treatment decision-making for UIAs.

Although exciting, there are several limitations to this study. First, the cause of altered metabolites and cytokines might be variable, as serum AA, OA, IL-1β, and TNF-α abnormalities might arise from other comorbidities. This could limit the generalizability of the results. However, many comorbidities and inflammatory conditions were excluded from this study. Second, patients were only longitudinally evaluated for 2 years. Hence, long-term aneurysm growth risk factor assessment requires future investigation. Third, this study only included Chinese patients, and whether these results would apply to other populations remains unclear. Fourth, this study just verified that the pharmacological intervention of OA, IL-1β, and TNF-α can prevent the rat model of IA from rupturing. The mechanisms of these phenomena were not discussed deeply. Fifth, AA usually could not be supplied by exogenous pure AA. Thus, whether the intervention of AA metabolism could prevent IA from rupture was ignored. Sixth, this study included limited clinical and radiological features, resulting in potential clinical and radiological features related to UIA instability, e.g., multiple aneurysms and wall enhancement. Despite the above limitations, this study revealed OA, AA, IL-1β, and TNF-α as biomarkers for UIA instability and presented the first risk stratification model based on radiological and multi-omics features. Further large cohorts with longer follow-up and multi-national studies should be conducted to verify the findings of this paper.

5. Conclusion

In this study, a multi-omics analysis was performed, and OA, AA, IL-1β, and TNF-α were revealed as biomarkers for UIA instability. This study developed a risk stratification model (instability classifier) incorporating radiological features and biomarkers with high accuracy to evaluate the 2-year risk of UIA instability, which may guide treatment decision-making for UIAs.

Conflict of interest

The authors declare that they have no conflict of interest.

Acknowledgments

This work was supported by the Top Talent Support Program for Medical Experts Team and for Young and Middle-Aged People of Wuxi Health Committee (202109 and 202014), the National Key R&D Program of China (2021YFC2501100 and 2020YFA0803700), and the National Natural Science Foundation of China (82071296, 81801158, and 81970425). We thank the participants of the study, and all clinical and research staff who contributed to the IARP-CP cohort and 100-Project cohort.

Author contributions

Conception and design: Qingyuan Liu, Ke Li, Hongwei He, Lemin Zheng, and Shuo Wang. Acquisition of data: Qingyuan Liu, Ke Li, Jun Wu, Shusi Ding, Zheng Wen, and Jiyuan Chen. Analysis and interpretation of data: Qingyuan Liu, Ke Li, and Zengli Miao. Drafting the article: Qingyuan Liu. Critically revising the article: Hongtu Cui, Jiangan Li, Shuo Wang, and Lemin Zheng. Reviewing submitted version of manuscript: all authors.

Appendix A. Supplementary materials

Supplementary materials to this article can be found online at https://doi.org/10.1016/j.scib.2023.05.001.

References

[1] Li MH, Chen SW, Li YD, et al. Prevalence of unruptured cerebral aneurysms in Chinese adults aged 35 to 75 years: a cross-sectional study. Ann Intern Med 2013;159:514–21.
[2] Thompson BG, Brown Jr RD, Amin-Hanjani S, et al. Guidelines for the management of patients with unruptured intracranial aneurysms: a guideline for healthcare professionals from the American Heart Association/American Stroke Association. Stroke 2015;46:2368–400.
[3] Korja M, Lehto H, Juvela S. Lifelong rupture risk of intracranial aneurysms depends on risk factors: a prospective Finnish cohort study. Stroke 2014;45:1958–63.
[4] Etminan N, Rinkel GJ. Unruptured intracranial aneurysms: development, rupture and preventive management. Nat Rev Neurol 2016;12:699–713.
[5] Algra AM, Lindgren A, Vergouwen MDI, et al. Procedural clinical complications, case-fatality risks, and risk factors in endovascular and neurosurgical treatment of unruptured intracranial aneurysms: a systematic review and meta-analysis. JAMA Neurol 2019;76:282–93.
[6] van der Kamp LT, Rinkel GJE, Verbaan D, et al. Risk of rupture after intracranial aneurysm growth. JAMA Neurol 2021;78:1228–35.
[7] Greving JP, Wermer MJ, Brown Jr RD, et al. Development of the phases score for prediction of risk of rupture of intracranial aneurysms: a pooled analysis of six prospective cohort studies. Lancet Neurol 2014;13:59–66.
[8] Backes D, Rinkel GJE, Greving JP, et al. Elapss score for prediction of risk of growth of unruptured intracranial aneurysms. Neurology 2017;88:1600–6.
[9] Cui H, Chen Y, Li K, et al. Untargeted metabolomics identifies succinate as a biomarker and therapeutic target in aortic aneurysm and dissection. Eur Heart J 2021;42:4373–85.
[10] Ma K, Yang J, Shao Y, et al. Therapeutic and prognostic significance of arachidonic acid in heart failure. Circ Res 2022;130:1056–71.
[11] Liu Q, Zhao J, Wang S. From cerebrovascular diseases to neuro-co-cardiological diseases: a challenge in the new epoch. Sci Bull 2022;67:1830–2.
[12] Frosen J, Tulamo R, Paetau A, et al. Saccular intracranial aneurysm: pathology and mechanisms. Acta Neuropathol 2012;123:773–86.
[13] Signorelli F, Sela S, Gesualdo L, et al. Hemodynamic stress, inflammation, and intracranial aneurysm development and rupture: a systematic review. World Neurosurg 2018;115:234–44.
[14] Frosen J, Piippo A, Paetau A, et al. Remodeling of saccular cerebral artery aneurysm wall is associated with rupture: histological analysis of 24 unruptured and 42 ruptured cases. Stroke 2004;35:2287–93.
[15] Liu Q, Zhang Y, Yang J, et al. The relationship of morphological-hemodynamic characteristics, inflammation, and remodeling of aneurysm wall in unruptured intracranial aneurysms. Transl Stroke Res 2021;13:88–99.
[16] Sun K, Zhang X, Li X, et al. Plasma metabolic signatures for intracranial aneurysm and its rupture identified by pseudotargeted metabolomics. Clin Chim Acta 2022;538:36–45.
[17] Koch M, Acharjee A, Ament Z, et al. Machine learning-driven metabolomic evaluation of cerebrospinal fluid: insights into poor outcomes after aneurysmal subarachnoid hemorrhage. Neurosurgery 2021;88:1003–11.
[18] Weng JC, Wang J, Li H, et al. Aspirin and growth of small unruptured intracranial aneurysm: results of a prospective cohort study. Stroke 2020;51:3045–54.
[19] Liu J, Xing H, Chen Y, et al. Rupture risk assessment for anterior communicating artery aneurysms using decision tree modeling. Front Cardiovasc Med 2022;9:900647.
[20] Xu T, Lin B, Liu S, et al. Larger size ratio associated with the rupture of very small (≤3 mm) anterior communicating artery aneurysms. J Neurointerv Surg 2017;9:278–82.
[21] Liu Q, Liu P, Zhang Y, et al. Serum interleukin-1 levels are associated with intracranial aneurysm instability. Transl Stroke Res 2023:1–15.
[22] Dhar S, Tremmel M, Mocco J, et al. Morphology parameters for intracranial aneurysm rupture risk assessment. Neurosurgery 2008;63:185–96.
[23] Baturynska I, Martinsen K. Prediction of geometry deviations in additive manufactured parts: comparison of linear regression with machine learning algorithms. J Intell Manuf 2021;32:179–200.
[24] Miyata H, Imai H, Koseki H, et al. Vasa vasorum formation is associated with rupture of intracranial aneurysms. J Neurosurg 2019;133:789–99.
[25] Oyama S, Ebina K, Etani Y, et al. A novel anti-TNF-alpha drug ozoralizumab rapidly distributes to inflamed joint tissues in a mouse model of collagen induced arthritis. Sci Rep 2022;12:18102.
[26] Hettwer J, Hinterdobler J, Miritsch B, et al. Interleukin-1beta suppression dampens inflammatory leucocyte production and uptake in atherosclerosis. Cardiovasc Res 2022;118:2778–91.
[27] Alba AC, Agoritsas T, Walsh M, et al. Discrimination and calibration of clinical prediction models: users' guides to the medical literature. JAMA 2017;318:1377–84.
[28] Hackenberg KAM, Rajabzadeh-Oghaz H, Dreier R, et al. Collagen turnover in relation to risk factors and hemodynamics in human intracranial aneurysms. Stroke 2020;51:1624–8.
[29] Liu P, Shi Y, Fan Z, et al. Inflammatory smooth muscle cells induce endothelial cell alterations to influence cerebral aneurysm progression via regulation of integrin and VEGF expression. Cell Transplant 2019;28:713–22.
[30] Moszak M, Szulinska M, Bogdanski P. You are what you eat-the relationship between diet, microbiota, and metabolic disorders-a review. Nutrients 2020;12:1096.
[31] Bjorkegren JLM. Lusis AJ. Atherosclerosis: recent developments. Cell 2022;185:1630–45.
[32] Cao H, Zhu Y, Hu G, et al. Gut microbiome and metabolites, the future direction of diagnosis and treatment of atherosclerosis? Pharmacol Res 2022;187:106586.
[33] Laval T, Chaumont L, Demangel C. Not too fat to fight: the emerging role of macrophage fatty acid metabolism in immunity to mycobacterium tuberculosis. Immunol Rev 2021;301:84–97.
[34] Mehta A, Shapiro MD. Apolipoproteins in vascular biology and atherosclerotic disease. Nat Rev Cardiol 2022;19:168–79.
[35] Jayaraj RL, Azimullah S, Beiram R, et al. Neuroinflammation: friend and foe for ischemic stroke. J Neuroinflammation 2019;16:142.
[36] Rink C, Khanna S. Significance of brain tissue oxygenation and the arachidonic acid cascade in stroke. Antioxid Redox Signal 2011;14:1889–903.
[37] Rodemerk J, Junker A, Chen B, et al. Pathophysiology of intracranial aneurysms: COX-2 expression, iron deposition in aneurysm wall, and correlation with magnetic resonance imaging. Stroke 2020;51:2505–13.
[38] Samson FP, Patrick AT, Fabunmi TE, et al. Oleic acid, cholesterol, and linoleic acid as angiogenesis initiators. ACS Omega 2020;5:20575–85.
[39] Meng H, Matthan NR, Wu D, et al. Comparison of diets enriched in stearic, oleic, and palmitic acids on inflammation, immune response, cardiometabolic risk factors, and fecal bile acid concentrations in mildly hypercholesterolemic postmenopausal women-randomized crossover trial. Am J Clin Nutr 2019;110:305–15.
[40] Furukawa H, Wada K, Tada Y, et al. Mast cell promotes the development of intracranial aneurysm rupture. Stroke 2020;51:3332–9.
[41] Dinarello CA. A clinical perspective of IL-1beta as the gatekeeper of inflammation. Eur J Immunol 2011;41:1203–17.
[42] Dinarello CA, Simon A, van der Meer JW. Treating inflammation by blocking interleukin-1 in a broad spectrum of diseases. Nat Rev Drug Discov 2012;11:633–52.
[43] Garlanda C, Dinarello CA, Mantovani A. The interleukin-1 family: back to the future. Immunity 2013;39:1003–18.
[44] Liu Q, Zhang Y, Zhu C, et al. Serum IL-1, pyroptosis and intracranial aneurysm wall enhancement: analysis integrating radiology, serum cytokines and histology. Front Cardiovasc Med 2022;9:818789.
[45] Moriwaki T, Takagi Y, Sadamasa N, et al. Impaired progression of cerebral aneurysms in interleukin-1beta-deficient mice. Stroke 2006;37:900–5.
[46] Starke RM, Raper DM, Ding D, et al. Tumor necrosis factor-alpha modulates cerebral aneurysm formation and rupture. Transl Stroke Res 2014;5:269–77.
[47] Kong P, Cui ZY, Huang XF, et al. Inflammation and atherosclerosis: signaling pathways and therapeutic intervention. Signal Transduct Target Ther 2022;7:131.
[48] Meng H, Tutino VM, Xiang J, et al. High WSS or low WSS? Complex interactions of hemodynamics with intracranial aneurysm initiation, growth, and rupture: toward a unifying hypothesis. AJNR Am J Neuroradiol 2014;35:1254–62.
[49] Zhang XJ, Gao BL, Hao WL, et al. Presence of anterior communicating artery aneurysm is associated with age, bifurcation angle, and vessel diameter. Stroke 2018;49:341–7.
[50] Wang Y, Cheng M, Liu S, et al. Shape related features of intracranial aneurysm are associated with rupture status in a large Chinese cohort. J Neurointerv Surg 2022;14:252–6.
[51] Liu Q, Leng X, Yang J, et al. Stability of unruptured intracranial aneurysms in the anterior circulation: nomogram models for risk assessment. J Neurosurg 2022;137:675–84.
[52] Bjorkman J, Frosen J, Tahtinen O, et al. Irregular shape identifies ruptured intracranial aneurysm in subarachnoid hemorrhage patients with multiple aneurysms. Stroke 2017;48:1986–9.

Qingyuan Liu is an M.D. candidate from Capital Medical University. His research mainly focuses on clinical characteristics, mechanisms, and treatment of intracranial aneurysm and intracerebral hemorrhage.

Ke Li is currently a Ph.D. candidate at the National Clinical Research Center of Neurological Diseases of Tiantan Hospital. His research mainly focuses on the diagnosis, treatment, and pathogenesis of cardiovascular and cerebrovascular diseases from a metabolomics perspective.

Xiaojie Lu is the academic leader in Neurosurgery at Jiangnan University Medical Center, and serves as the deputy director of the Neuroendoscope Committee of the Chinese Medical Doctor Association. His research interest mainly includes the clinical and translational research of endoscopic minimally invasive neurosurgery.

Jiangan Li is the vice director of the Emergency Department, Jiangnan University Medical Center. His research mainly focuses on the basic and clinical research of glioma and cerebrovascular diseases.

Lemin Zheng is a principal investigator of the National Key Laboratory of Vascular Homeostasis and Remodeling, Peking University, the vice director of Peking University Institute of Cardiovascular Sciences, and director of the Laboratory of Cardiovascular Metabolism. His research mainly focuses on cardiovascular and cerebrovascular diseases and their translational research and metabolic-related diseases.

Shuo Wang is a principal investigator of the National Clinical Research Center for Neurological Diseases, and the vice director of Neurosurgical College of Capital Medical University. As the chairman of the Neurosurgery Branch of the Chinese Medication Association and the Cerebrovascular Surgery Branch of the Chinese Stroke Association, he mainly focuses on surgical treatment and the mechanism of cerebrovascular diseases.